Supplemental material to: "Density and spin response of a strongly-interacting Fermi gas in the attractive and quasi-repulsive regime"

F. Palestini, P. Pieri, and G. C. Strinati
Physics Division, School of Science and Technology
University of Camerino, I-62032 Camerino (MC), Italy

Diagrammatic formalism and linear response

The number density

$$\rho(\mathbf{r}) = \sum_{\alpha} \psi^{\dagger}_{\alpha}(\mathbf{r})\, \psi_{\alpha}(\mathbf{r}) \tag{1}$$

and spin density ($\hbar = 1$)

$$S_z(\mathbf{r}) = \frac{1}{2} \sum_{\alpha,\beta} \psi^{\dagger}_{\alpha}(\mathbf{r})\, \sigma^{(z)}_{\alpha\beta}\, \psi_{\beta}(\mathbf{r}) \tag{2}$$

operators, where $\sigma^{(z)}$ is a Pauli matrix, are expressed in terms of the fermionic field operator $\psi_{\alpha}(\mathbf{r})$ at space point $\mathbf{r}$ and with spin index $\alpha = (\uparrow, \downarrow)$. In terms of these operators, one writes the density-density

$$\chi_n(\mathbf{r}\tau, \mathbf{r}'\tau') = -\langle T_{\tau}\, [\rho(\mathbf{r}\tau)\rho(\mathbf{r}'\tau')]\rangle \tag{3}$$

and spin-spin

$$\chi_s(\mathbf{r}\tau, \mathbf{r}'\tau') = -\langle T_{\tau}\, [S_z(\mathbf{r}\tau) S_z(\mathbf{r}'\tau')]\rangle \tag{4}$$

correlation functions with imaginary time τ. Here, T_{τ} is the time-ordering operator and

$$\psi^{\dagger}_{\alpha}(\mathbf{r}\tau^{+})\, \psi_{\beta}(\mathbf{r}\tau) = e^{(H-\mu N)\tau} \psi^{\dagger}_{\alpha}(\mathbf{r})\, \psi_{\beta}(\mathbf{r}) e^{-(H-\mu N)\tau} \tag{5}$$

is a modified Heisenberg picture with Hamiltonian H, number operator N, and chemical potential μ. Accordingly, in Eqs.(3) and (4) the symbol $\langle \cdots \rangle$ corresponds to a grand-canonical average [1]. The correlation functions (3) and (4) represent particular cases of the two-particle correlation function [2].

From the above expressions, for a homogeneous system the (isothermal) compressibility χ_n and spin susceptibility χ_s follow as the static limits:

$$\chi_n = \left.\frac{\partial n}{\partial \mu}\right|_T = \lim_{\mathbf{q}\to 0} \chi_n(\mathbf{q}, \Omega_{\nu} = 0) \tag{6}$$

$$\chi_s = \left.\frac{\partial M}{\partial h}\right|_T = \lim_{\mathbf{q}\to 0} \chi_s(\mathbf{q}, \Omega_{\nu} = 0) \tag{7}$$

where n is the density, M the magnetization, h a uniform magnetic field, and

$$\chi_{n/s}(\mathbf{q}, \Omega_{\nu}) = \int_0^{1/(k_B T)} d(\tau - \tau')\, e^{i\Omega_{\nu}(\tau - \tau')} \times \int d(\mathbf{r} - \mathbf{r}')\, e^{-i\mathbf{q}\cdot(\mathbf{r} - \mathbf{r}')}\, \chi_{n/s}(\mathbf{r}\tau, \mathbf{r}'\tau')\,. \tag{8}$$

Here, $\mathbf{q}$ is a wave vector, $\Omega_{\nu} = 2\pi\nu T$ (ν integer) a bosonic Matsubara frequency, and k_B the Boltzmann constant. The values of the static limits (6) and (7) can conveniently be normalized in terms of the corresponding non-interacting values $2N_0$ and $2N_0\mu_B^2$, in the order, where $N_0 = mk_F/(2\pi)^2$ is the density of states per spin component and μ_B the Bohr magneton.

Standard diagrammatic methods can be used to calculate the correlation functions $\chi_n(\mathbf{q}, \Omega_{\nu})$ and $\chi_s(\mathbf{q}, \Omega_{\nu})$ in Fourier space [1], both in the normal phase above T_c and in the superfluid phase below T_c.

Choice of diagrams for compressibility and spin susceptibility

Above T_c, a pairing-fluctuation approach that extends the Galitskii theory [3] throughout the BCS-BEC crossover [4] identifies the relevant fermionic single-particle self-energy $\Sigma_{\rm L}$ with the diagram depicted in the upper panel of Fig.S1, where the particle-particle (ladder) propagator Γ_0 is depicted in the lower panel of the same figure. It sums up all the elementary scattering processes between two fermions propagating in the medium with opposite spins owing to the contact nature of the inter-particle interaction.

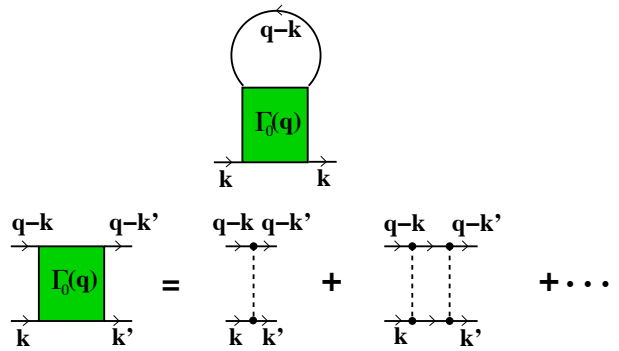

FIG. S1. Single-particle fermionic self-energy in the normal phase (upper panel) expressed in terms of the ladder propagator Γ_0 between two fermions of opposite spins (lower panel). Full and dashed lines represent the fermionic propagator and interaction potential.

The two-particle response that bears on this self-energy contains the effective two-particle interaction of the kinds depicted in Fig.S2 (that corresponds to Fig.3 of Ref.[5]). To the lowest order, these terms produce the Aslamazov-Larkin (AL) diagram of Fig.1(c) plus its twisted companion of Fig.1(d) of the main text, and the Maki-Thompson

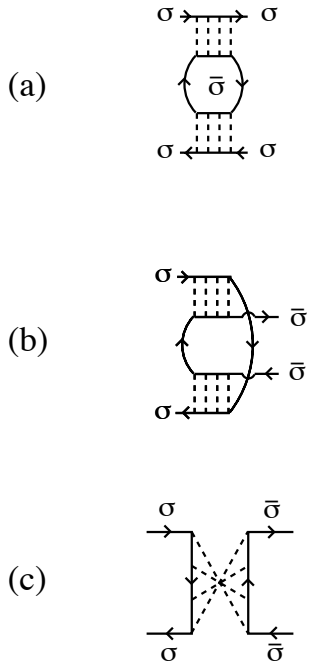

FIG. S2. The three types of effective two-particle interaction obtained from the pairing self-energy of Fig.S1, which give rise to the AL, twisted AL, and MT diagrams of Fig.1 of the main text, in the order.

(MT) diagram of Fig.1(b) of the main text. The two AL diagrams give equal contribution to the compressibility, but cancel each other for the spin susceptibility owing to the spin structure. On the other hand, the DOS diagram of Fig.1(a) of the main text, where the above effective two-particle interaction does not appear, and the MT diagram of Fig.1(b) of the main text contribute to both quantities. This justifies the choice of diagrams made in the main text.

Repeated structures based on the effective two-particle interactions of Fig.S2 are also possible, and are specifically required by general conservation requirements [6]. Along these lines, for the calculation of the compressibility we have included the series of modified AL diagrams whose lowest-order contribution is depicted in Fig.1(e) of the main text. In this case, these repeated processes are important on physical grounds because they generalize to the BCS-BEC crossover analogous processes occurring for point-like bosons in the normal phase at the Hartree-Fock level, where they introduce the effects of the mutual repulsion between bosons and thus prevent the compressibility from diverging when approaching T_c from above.

In practice, in the static limit it is possible to include this whole series of physical processes by exploiting a Ward identity that connects single- and two-particle fermionic Green's functions [7], whereby summing the whole series of modified AL diagrams is equivalent to calculating numerically $\partial n/\partial\mu$ in the following way. The

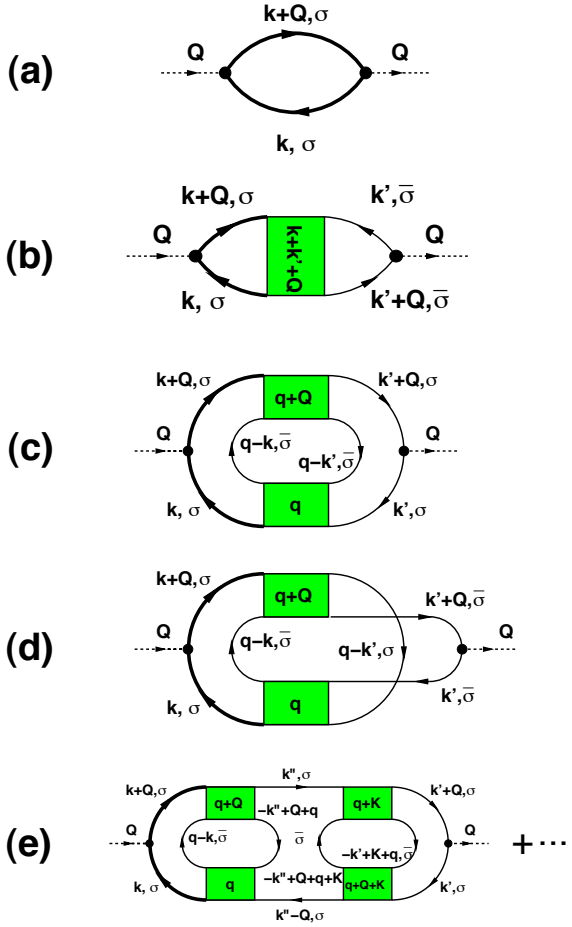

FIG. S3. The diagrams of Fig.1 of the main text are reproduced here with two thick lines each, which represent fermionic propagators dressed self-energy insertions. This dressing of the fermionic lines results when calculating the compressibility as $\chi_n = \partial n/\partial\mu$ and the spin susceptibility as $\chi_s = \partial M/\partial h$ through Ward identities.

density is obtained from the expression

$$n = 2\,k_B T \sum_n e^{i\omega_n \eta} \int \frac{d\mathbf{k}}{(2\pi)^3}\, G(\mathbf{k},\omega_n) \qquad (9)$$

in terms of the fermionic single-particle Green's function $G(\mathbf{k},\omega_n) = [i\omega_n - \mathbf{k}^2/(2m) + \mu - \Sigma_{\rm P}(\mathbf{k},\omega_n)]^{-1}$ where $\mathbf{k}$ is a wave vector, $\omega_n = \pi k_B T(2n+1)$ (n integer) a fermionic Matsubara frequency, and η a positive infinitesimal. The fermionic self-energy $\Sigma_{\rm P}$ is formally of the type of $\Sigma_{\rm L}$ of Fig.S1, but with a dressed ladder propagator Γ that replaces Γ_0 in order to include interaction processes between composite bosons as described by the generalized Popov theory of Ref.[8].

A comment is in order at this point about the degree of self-consistency that results when the diagrammatic structure for χ_n is generated in the above way by taking the derivative of the expression (9) for n with respect to μ. One formally obtains the same diagrams of

Fig.1 of the main text that contribute to χ_n (namely, diagrams (a), (c), (d) and the whole series (e)), but now with two fermionic propagators (identified by the thick lines in Fig.S3) which are dressed by the self-energy $\Sigma_{\rm P}$.

Below T_c, the calculation of the spin-spin correlation function can initially be done at the level of the BCS (mean-field) approximation, whereby the bare bubble of Fig.1(a) of the main text is replaced by the sum of two bubbles calculated, respectively, with two normal (G_{11}) and two anomalous (G_{12}) single-particle Green's functions [9]. In particular, in the static limit one obtains for the spin susceptibility at the BCS level [10]:

$$\frac{\chi_s^{(BCS)}(T)}{2N_0\mu_B^2} = -\frac{1}{N_0}\int \frac{d\mathbf{k}}{(2\pi)^3}\frac{\partial f_F(E_\mathbf{k})}{\partial E_\mathbf{k}} \qquad (10)$$

where $E_\mathbf{k} = [(\mathbf{k}^2/(2m)-\mu)^2+|\Delta|^2]^{1/2}$ is the BCS dispersion with gap Δ and $f_F(E) = (e^{E/(k_BT)}+1)^{-1}$ the Fermi function. Note that this quantity vanishes in the zero-temperature limit, reflecting the singlet structure of the Cooper pairs. The mechanism for this to occur is a cancellation of the contributions of the normal and anomalous BCS bubbles.

Pairing fluctuations beyond mean field can be included below T_c following the approach of Ref.[11]. In particular, in the above two BCS (bubble) diagrams for the spin-spin correlation function the normal single-particle Green's functions G_{11} are affected by pairing fluctuations while the anomalous ones G_{12} remain at the BCS level. In addition, the MT diagram of Fig.1(b) of the main text is introduced where now all single-particle lines are G_{11}. In this way one recovers the vanishing of the spin susceptibility at zero temperature for any coupling $(k_Fa_F)^{-1}$.

Above T_c, on the other hand, for the spin-spin correlation function the DOS diagram replaces the normal BCS bubble while the MT diagram plays the role of the anomalous BCS bubble. In this case, a complete cancellation between the MT diagram and the fluctuation contributions to the DOS diagram occurs in the strong-coupling (BEC) limit for temperatures well below the pair-breaking temperature of the composite bosons. This is expected on physical grounds, since a non-vanishing contribution to the spin response for spin-less composite bosons should result only when the temperature is comparable with their binding energy and the composite bosons break apart [5].

A comment on the degree of self-consistency for the diagrammatic structure is relevant also for χ_s. At the BCS level, no difference is introduced when calculating χ_s via $\partial M/\partial h$ with respect to the diagrammatic calculation resulting in the expression (10). When fluctuations are introduced, while both fermionic propagators of the DOS diagram of Fig.1(a) of the main text are affected by pairing fluctuations, only the pair of fermionic propagators on the left side of the MT diagram of Fig.1(b) of the main text are dressed by pairing fluctuations through the self-energy $\Sigma_{\rm L}$ depicted in Fig.S1, both above and below T_c. This corresponds to the occurrence of thick lines in panels (a) and (b) of Fig.S3. We have, however, verified numerically that the dressing S3(b) of the MT diagram does not affect our main physical results, namely, that χ_s is strongly suppressed for $T \ll T_c$ and vanishes at $T = 0$, while it slowly decreases for increasing temperature when $T \gtrsim T_F$ where it coincides with the results of the high-temperature (virial) expansion.

[1] A. L. Fetter and J. D. Walecka, *Quantum Theory of Many-Particle Systems* (McGraw-Hill, New York, 1971).
[2] G. Strinati, Rivista Del Nuovo Cimento **11**, 1 (1988).
[3] V. M. Galitskii, Sov. Phys. JETP **7**, 104 (1958).
[4] P. Pieri and G. C. Strinati, Phys. Rev. B **61**, 15370 (2000).
[5] G. C. Strinati, P. Pieri, and C. Lucheroni, Eur. Phys. J. B **30**, 161 (2002).
[6] G. Baym, Phys. Rev. **127**, 1391 (1962).
[7] E. M. Lifshitz and L. P. Pitaevskii, *Statistical Physics, Part 2* (Butterworth-Heinemann, Oxford, 2006), Section 19.
[8] P. Pieri and G. C. Strinati, Phys. Rev. B **71**, 094520 (2005).
[9] G. D. Mahan, *Many-Particle Physics* (Plenum Press, New York, 1981) Section 10.5.
[10] K. Yosida, Phys. Rev. **110**, 769 (1958).
[11] P. Pieri, L. Pisani, and G. C. Strinati, Phys. Rev. B **70**, 094508 (2004).